Experimental Brain Research (2019) 237:1397–1407
https://doi.org/10.1007/s00221-019-05521-2

RESEARCH ARTICLE

c-Fos expression in the limbic thalamus following thermoregulatory and wake–sleep changes in the rat

Marco Luppi[1] · Matteo Cerri[1] · Alessia Di Cristoforo[1] · Timna Hitrec[1] · Daniela Dentico[2,6] · Flavia Del Vecchio[1,3] · Davide Martelli[1,4] · Emanuele Perez[1] · Domenico Tupone[1,5] · Giovanni Zamboni[1] · Roberto Amici[1]

Received: 9 November 2018 / Accepted: 13 March 2019 / Published online: 18 March 2019

Abstract

A cellular degeneration of two thalamic nuclei belonging to the "limbic thalamus", i.e., the anteroventral (AV) and mediodorsal (MD) nuclei, has been shown in patients suffering from Fatal Familial Insomnia (FFI), a lethal prion disease characterized by autonomic activation and severe insomnia. To better assess the physiological role of these nuclei in autonomic and sleep regulation, c-Fos expression was measured in rats during a prolonged exposure to low ambient temperature (T_a, − 10 °C) and in the first hours of the subsequent recovery period at normal laboratory T_a (25 °C). Under this protocol, the thermoregulatory and autonomic activation led to a tonic increase in waking and to a reciprocal depression in sleep occurrence, which was more evident for REM sleep. These effects were followed by a clear REM sleep rebound and by a rebound of Delta power during non-REM sleep in the following recovery period. In the anterior thalamic nuclei, c-Fos expression was (1) larger during the activity rather than the rest period in the baseline; (2) clamped at a level in-between the normal daily variation during cold exposure; (3) not significantly affected during the recovery period in comparison to the time-matched baseline. No significant changes were observed in either the MD or the paraventricular thalamic nucleus, which is also part of the limbic thalamus. The observed changes in the activity of the anterior thalamic nuclei appear, therefore, to be more specifically related to behavioral activation than to autonomic or sleep regulation.

Keywords Fatal familial insomnia · Sleep deprivation · Cold exposure · Autonomic regulation · P-CREB

Abbreviations

AD	Anterodorsal thalamic nuclei
AOI	Areas of interest
AV	Anteroventral thalamic nuclei
C24	Control experimental condition, starting at 9 AM 24 h at n-lab Ta
C5	Control experimental condition, starting at 9 AM 5 h at n-lab Ta
DAB	3,3′-Diaminobenzidine tetrahydrochloride
E24	Exposure experimental condition, starting at 9 AM 24 h at − 10 °C
E48	Exposure experimental condition, starting at 9 AM 48 h at − 10 °C
E5	Exposure experimental condition, starting at 9 AM 5 h at − 10 °C
EEG	Electroencephalography
FFI	Fatal familial insomnia
HSI	Hue–saturation–intensity digital system
IPA	Image Pro Analyzer software
IRNs	Immunoreactive neurons
LD	Light–dark
MA	Motor activity
MD	Mediodorsal thalamic nuclei

✉ Marco Luppi
marco.luppi@unibo.it

[1] Department of Biomedical and NeuroMotor Sciences, University of Bologna, Piazza di Porta San Donato, 2, 40126 Bologna, Italy

[2] University of Wisconsin-Madison, 625 W. Washington Ave., Madison, WI 53703-2637, USA

[3] Present Address: Institut de Recherche Biomédicale des Armées, Unité Risques Technologiques Emergents, BP73, 91223 Bretigny/Orge Cedex, France

[4] Florey Institute of Neuroscience and Mental Health, University of Melbourne, Parkville, VIC 3010, Australia

[5] Department of Neurological Surgery, Oregon Health and Science University, Portland, OR, USA

[6] Present Address: Dipartimento Interateneo di Fisica, Università degli Studi "Aldo Moro" di Bari, Bari, Italy

MnPO	Median preoptic nucleus of the hypothalamus
n-lab Ta	Normal laboratory ambient temperature (i.e., 25.0 ± 1.0 °C)
NREMS	Non-REM sleep
P-CREB	Phosphorylated cAMP-response-element-binding-protein
PVN	Paraventricular thalamic nucleus
R5-E24	Recovery experimental condition, starting at 9 AM 5 h at n-lab T_a following 24 h at − 10 °C
R5-E24	Recovery experimental condition, starting at 9 AM 5 h at n-lab T_a following 48 h at − 10 °C
REM	Rapid-eye movement
REMS	REM sleep
T_a	Ambient temperature
Thy	Hypothalamic temperature
VA	Ventral anterior thalamic nuclei
VLPO	Ventrolateral preoptic nucleus of the hypothalamus
WS	Wake–sleep

Introduction

Central nervous somatic and autonomic regulation of bodily functions undergoes deep and complex functional changes throughout the different wake–sleep (WS) states (Parmeggiani 2003; Luppi et al. 2010; Amici et al. 2014; Martelli et al. 2014). Consequently, physiological challenges that activate central regulatory mechanisms lead to privilege the occurrence of the WS state which has the more appropriate somatic and autonomic regulatory capacity. Accordingly, thermoregulatory and autonomic activation prompted by the exposure to low ambient temperature (T_a) leads, in mammals, to an increase in waking and a disruption of sleep that are directly related to the extent T_a is set below the lower critical limit of the thermoneutral zone of the species (Amici et al. 2008, 2014; Parmeggiani 2003).

In our lab, the severe sleep disruption caused in the rat by the exposure to a very low T_a (− 10 °C) (Amici et al. 2008; Cerri et al. 2005) has been related to the activity of the median preoptic nucleus (MnPO) and the ventrolateral preoptic nucleus (VLPO) of the hypothalamus, two areas deeply involved in the central nervous control of autonomic and WS regulation (Szymusiak et al. 1998; Zamboni et al. 2004; McKinley et al. 2015), by determining the immunoreactivity levels of both c-Fos and the phosphorylated cAMP-response-element-binding-protein (P-CREB) (Dentico et al. 2009). The results showed that c-Fos expression was increased in these nuclei during a 24 and 48-h exposure to T_a − 10 °C and during the following recovery, carried out by returning animals at normal laboratory (n-lab) Ta, that was characterized by a large REM sleep (REMS) rebound and a rebound of Delta power during non-REM sleep (NREMS) in the following recovery period (Dentico et al. 2009).

In humans, a severe sleep disruption associated with a circadian dysregulation and an increase in sympathetic tone, concomitant with hypertension, tachycardia and hyperthermia, has been described in Fatal Familial Insomnia (FFI), a prion disease leading patients to death (Lugaresi et al. 1986, 1998; Montagna et al. 1998). Although characterized by focal lesions at the cortical and subcortical level, varying in intensity with the duration of the disease, FFI is considered a "preferential thalamic degeneration" in which the antero-ventral (AV) and medio-dorsal (MD) thalamic nuclei are invariably affected by a precocious and large cell loss (Parchi et al. 1998). The association between the neuropathological findings and main symptoms of the disease led to the hypothesis that both AV and MD might play a role in the processes underlying autonomic and WS regulation (Montagna et al. 2003).

Both AV and MD belong to the limbic subdivision of the thalamus (Vertes et al. 2015), which they, respectively, connect to the hippocampus–mesencephalon and the frontal cortex–basolateral amygdala by which they appear to play, in rodents, different roles consisting in performing tasks related to spatial memory and in ascribing meanings to incoming information (Wolff et al. 2015). In this line of thinking, the dysautonomia and sleep disturbances observed in FFI have been mainly referred to MD because of its connections with autonomic and WS-regulatory areas (Benarroch 1993; Velajos et al. 1998; Vertes et al. 2015).

However, the experimental evidence of a physiological involvement of AV and MD in central autonomic control and/or WS regulation is rather poor. For example, in the rat, the pharmacological disinhibition of MD led to an increase in heart rate and blood pressure in rats (Stotz-Potter and Benarroch 1998). Moreover, in cats, the discharge pattern of MD neurons has been shown to be wake–sleep related, and the mean frequency rate to be lower in REMS compared to Wake (Imeri et al. 1988). However, the bilateral lesion of MD only transitorily depressed both non-REM sleep and REM sleep occurrence (Marini et al. 1988a, b). Furthermore, wide bilateral lesions of the anterior thalamic nuclei produced, in the rat, postural deficits, but not relevant WS changes (van Groen et al. 2002).

In the rat, the sleep disruption caused by the exposure to T_a − 10 °C is concomitant with an activation of sympathetic premotor neurons, located in the brainstem, within the rostral raphe pallidus (Morrison 2016), which promote cutaneous vasoconstriction and both shivering and non-shivering thermogenesis. On this basis, the experimental paradigm, formed by a prolonged exposure to T_a − 10 °C and the following return to n-lab Ta, may be considered a suitable model for the assessment of the physiological role of AV and MD in autonomic and WS regulation. To this aim,

the same brain sections that were taken and fully digitalized in our previous study (Dentico et al. 2009) were further scrutinized. This analysis concerned AV and MD and two other nuclei of the limbic thalamus (Vertes et al. 2015): (1) the antero-dorsal (AD), adjacent to and functionally related with AV (van Groen et al. 2002; Tsanov et al. 2011; Sheroziya and Timofeev 2014); (2) the paraventricular (PVN), which is thought to play a role in visceral awareness for its large monoaminergic input and for its output to the prefrontal cortex (Benarroch and Stotz-Potter 1998; Van der Werf et al. 2002). Furthermore, the ventral anterior (VA) nucleus, a relay thalamic nucleus mostly involved in somatomotor control (Steriade et al. 1997; Garcia-Munoz and Arbuthnott 2015), was also assessed to evaluate the possible stimulatory role of the behavioral activation induced by the adaptive response to changes in ambient conditions (Jankowsky et al. 2013).

Methods and materials

Animals

Male Sprague–Dawley rats (201–225 g; Charles River) were used. Animals were acclimated to n-lab T_a (25.0 ± 1.0 °C) and to a 12 h:12 h light–dark (LD) cycle (L: 09:00–21:00; 100–150 lx at cage level); food and water were ad libitum. The results of the present study come from a further analysis of the samples that were previously collected, but only partly analyzed (Dentico et al. 2009). These experiments were approved by the Ethical Committee of the University of Bologna under the supervision of the National Health Authority (Ministero della Sanità) in accordance with the European Union Directive (86/609/EEC; DLGS 27/01/1992 No. 116, Italy). Animal care was under the direct control of the University Veterinary Service.

Experimental procedure

The experimental procedure was described in a previous paper (Dentico et al. 2009). The experiment was carried out on two separate groups of animals by means of two experimental approaches: one behavioral, studying the changes in the WS cycle, and the other immunohistochemical, studying cFos and P-CREB expression at thalamic level.

Wake–sleep study

As previously described (Dentico et al. 2009), ten animals adapted to n-lab T_a (i.e., 25 ± 1.0 °C) and to a 12h:12 h light–dark (LD) cycle (Light on: 09:00) were implanted under general anesthesia (diazepam, Valium, Roche, 5 mg/kg, i.m. ketamine-HCl, Ketalar, Parke-Davis 100 mg/kg, i.p.) with: (1) two stainless steel epidural electrodes for electroencephalographic (EEG) recording; (2) a thermistor (B10KA303N, Thermometrics, Parthenia St. Northridge, CA) to measure hypothalamic temperature (Thy). The plugs were embedded in acrylic dental resin, which was anchored to the skull by small stainless steel screws. Following at least a 1-week recovery from surgery, rats were placed in Plexiglas cages within a thermoregulated and sound-attenuated box that was located in a sound-attenuated room. EEG, Thy and the motor activity (MA) of each animal were continuously recorded during five consecutive 24-h sessions starting at Light on. Following 2 days of recording for the baseline, animals were exposed for 48 h to T_a − 10.0 ± 1.0 °C, and then allowed to recover at n-Lab Ta.

During the recordings, the EEG signal was amplified, filtered (high-pass filter: − 40 dB at 0.35 Hz; low-pass filter: − 6 dB at 60 Hz; digital Notch filter: − 40 dB at 50 Hz) and after analog-to-digital conversion (sampling rate: EEG, 128 Hz) stored on a PC. The EEG signal was subjected to on-line Fast Fourier Transform (FFT) and EEG power values were obtained for 4-s epochs in the Delta (0.75–4.0 Hz), Theta (5.5–9.0 Hz), and Sigma (11.0–16.0 Hz) band. Thy signal was amplified (1 °C /1 V) before analog-to-digital conversion (sampling rate: 8 Hz). MA was monitored by means of a passive infrared detector (Siemens, PID10, Munich, FRG) placed at the top of each cage. The signal was amplified and integrated before analog-to-digital conversion (sampling rate: 8 Hz), to make the output proportional to the amplitude and the duration of movement.

WS parameters were assessed by means of user software (QuickBASIC). EEG, Thy, and MA signals were visually scored to determine the beginning and end of each REMS episode according to criteria previously described (Cerri et al. 2005). A REMS episode was considered to have begun only if the EEG changes associated with this sleep stage were concomitant with an increase in Thy, and considered to be over only if the EEG and postural changes were associated with a decrease in Thy. The time for the minimal duration of a REMS episode was fixed at 8 s. Following the removal of REMS epochs and that of the 4-s epochs that showed EEG artifacts, an automatic procedure was used to separate Wake from NREMS (Cerri et al. 2005).

Statistical analysis Statistical analysis was carried out by means of Repeated Measure ANOVA (SPSS 23.0). Significance levels were pre-set at $P < 0.05$ and determined by means of the modified t statistics (t^*). A number of preplanned orthogonal and non-orthogonal comparisons were carried on. For the only non-orthogonal comparisons, significant levels were corrected according to the sequential Bonferroni's method (Holm 1979; Wallenstein et al. 1980).

Immunohistochemical study

Briefly, animals were individually housed 24 h before the start of the experimental session. Each session started at Light onset (09:00 h). Animals were randomly assigned to one of the following seven experimental conditions:

1. two Control conditions, in which animals were killed at n-lab Ta, at either Light onset (C24, $n=3$) or 5 h later (C5, $n=4$), to match the timing of the sampling of the five treatment conditions;
2. three Cold-Exposure conditions, in which animals were kept for either 5 h (E5, $n=3$), 24 h (E24, $n=3$), or 48 h (E48, $n=3$) at low T_a (-10.0 ± 1.0 °C);
3. two Recovery conditions, in which animals were allowed to spend 5 h at n-lab T_a after either a 24 h (R5-E24, $n=4$) or a 48 h (R5-E48, $n=4$) exposure to low Ta.

However, the number of cases per condition was reduced from four to three for the C5, R5-E24, and R5-E48 experimental groups since in one animal from each group the sections corresponding to the thalamic structures were absent or damaged. Thus, with respect to the study during which the images were taken and digitalized (Dentico et al. 2009), in the present paper, the final size of each experimental group was taken to $n=3$.

At the end of each experimental session, rats were sacrificed under diethyl-ether anesthesia by intra-aortic perfusion with 300 ml of a 4% (w/v) paraformaldehyde cold (4 °C) solution, preceded by a wash with 100 ml of cold 0.01 M PBS. Brains were post-fixed in 4% paraformaldehyde at 4 °C for 4–6 h.

Immunohistochemistry

The immunohistochemistry procedure was described in a previous paper (Dentico et al. 2009). Briefly, following 60–72 h of immersion in a 20% sucrose solution for cryoprotection, brains were quickly frozen at − 80 °C. Consecutive coronal sections were cut at 40 µm in a cryostat (Frigocut, Reichert-Jung, cf. Leica Microsystems Nussloch GmbH, Wetzlar, Germany) at − 21 °C. Sections were processed as follows: one out of every five was stained with Cresyl Violet for the anatomical recognition; the other four out of the five were alternately processed for c-Fos and P-CREB immunohistochemistry so that two sections out of five were stained for c-Fos antigen and two for P-CREB antigen. For the immunohistochemical stainings, free floating sections were incubated with a rabbit anti-c-Fos primary antiserum (Ab-5, Calbiochem, La Jolla, CA; 1: 20,000) or a rabbit anti-P-CREB immunopurified IgG (Upstate, Lake Placid, NY; 1:1000) on a shaking table for 72 or 48 h, respectively, at 4 °C.

Sections were then incubated with a biotinylated goat anti-rabbit IgG (Vector Laboratories, Burlingame, CA; 1:200) for 2 h at room temperature and subsequently reacted with biotinylated horseradish peroxidase pre-incubated with avidin (AB complex, Vector Vectastain ABC kit Standard; 1:100) and developed with 3,3′-diaminobenzidine (DAB) tetrahydrochloride (Sigma- Aldrich, St. Louis, MO; 0.05 mg/100 ml) to produce a brown reaction product in cell nuclei. After the staining, the sections were mounted on gelatinized slides, dehydrated through graded alcohol, and coverslipped with DPX mountant.

Quantification of the immunoreaction

The following procedure was used to count both c-Fos- and P-CREB-positive cell nuclei. Only coronal sections between − 1.7 and − 2.3 mm from bregma (Paxinos and Watson 2007) were considered for the analysis since specifically within these levels all the analyzed nuclei were contemporaneously present on the same section. Images were digitally scanned at a final magnification of 20 ×, by means of a whole slide imaging scanner (Hamamatsu Photonics, Milan, Italy), which was rented at the Company Immagini&Computer (Milan, Italy). All images were automatically calibrated on the background when scanned. The images were analyzed blindly using Image Pro Analyzer 7.0 (IPA, Media Cybernetics) software, without applying any adjustment for brightness or contrast. Since the high-definition images obtained were extremely large (i.e., about 3 GB each), to make the image analysis possible for the IPA software, only the thalamic area of the coronal section was extracted from each of the whole slide high-definition image as a TIFF image and analyzed, as shown in Fig. 1. This step was possible by means of a customized program running in IPA, specifically developed by Immagini&Computer for our laboratory.

Since the definition of the positive-stained nuclei was based on the gray intensity (see later in the text), the counting procedure was carried on considering the only "Intensity" channel of the HSI (i.e., hue–saturation–intensity) digital system. This channel was extracted from the original thalamic image in IPA; the result was a simple black/white image (Fig. 1b), in which every pixel was represented by the only intensity information, on a 256 levels scale in which the value "0" is total black and value "255" is total white.

Areas of interest (AOI), delimiting each single thalamic nucleus analyzed, were manually drawn by the experimenter, as shown in Fig. 2. As shown in the figure, the manual drawing was made comparing the slide image with the corresponding figure on the brain atlas (Paxinos and Watson 2007). For each image, the following nine AOI were drawn and saved for subsequent analyses: VA (left and right), AV

Fig. 1 Image acquisition and pre-analysis elaboration. In **a**, a digitally scanned example of the whole coronal brain section is shown, stained for c-Fos; the rectangle within the picture represents the area analyzed, extracted in high-definition from the original file. In **b**, the corresponding analyzed area is shown, following the extraction of the "intensity" channel from the HSI (hue–saturation–intensity) digital system. In **c**, an equivalent image from a brain section stained for P-CREB is shown. Scale bars are 1 mm

(left and right), AD (left and right), MD (left and right) and PVN.

Counting of the positive nuclei was carried on automatically, using specific and consolidated IPA functions, opportunely set up. In particular, considering the intensity scale, the positive threshold value and the stained area filter were defined as in Dentico et al. (2009). To avoid counting of some artifact dye staining, two kinds of "shape filters" of the counted objects were additionally introduced: (1) the "Aspect" filter was set within the range of 1–4, this filter is based on the ratio between major axis and minor axis of each stained object; (2) the "Roundness" filter was set within the range of 1–3, this filter is based on the ratio between actual circumference of the stained object and theoretical circumference, which was calculated from the stained area as it was a circle. Thanks to the overall regular shape of the neuronal cell nuclei stained with DAB, all those "shape filters" made it possible to discard unwanted objects from the automatic counting (Fig. 3). Finally, by means of another specific and consolidated IPA function, it was possible to split nuclei clusters into singularities, to not underestimate the counting value, due to the clustering of nearby or superimposed positive cell nuclei (Fig. 3). Finally, the area of each single AOI drawn was measured and counts were normalized for an area of 100μm^2.

Within the neuroanatomical limits considered, the number of sections counted for each rat and for both antigens, ranged from two to four. Also, cell counts were made bilaterally, excluding the PVN as the only median structure considered. Since no significant differences (see later in the text) were found between left and right nuclei of all the bilateral thalamic structures analyzed, all counting values were averaged to yield a single value for each thalamic nucleus, rat and antigen.

Statistical analysis

Statistical analysis was carried out by means of SPSS 23.0. Results were evaluated by means of univariate analysis of variance (ANOVA). Between-group factor had seven levels (C5, C24, E24, E48, E5, R5-E24, and R5-E48) for all nuclei. For each nucleus, antigens were analyzed separately.

Pre-planned orthogonal contrasts were carried out according to the following: (1) (E24/ E48) vs C24; (2) E48 vs E24; (3) E5 vs C5; (4) R5-E48 vs R5-E24. Pre-planned non-orthogonal comparisons were carried out according to the following: (1) C5 vs C24; (2) E24 vs C24; (3) E48 vs C24;

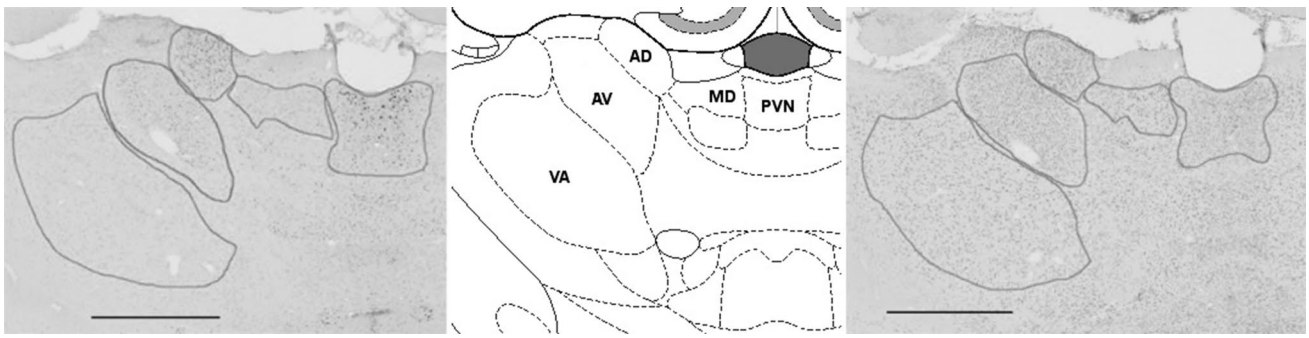

Fig. 2 Definition of the areas of interest. The figure shows the manual definition of the different areas of interest (AOI, in grey), hand-drawn by the experimenter. The AOI were defined by directly comparing images with the corresponding anatomical level of the rat brain atlas (middle figure). On the left, an example of a c-Fos-stained coronal section of the brain is shown, while on the right there is an example of the P-CREB-stained equivalent section. Both section pictures represent only the "intensity" channel of the HSI (hue–saturation–intensity) digital system, extracted from the original picture. Scale bars are 1 mm

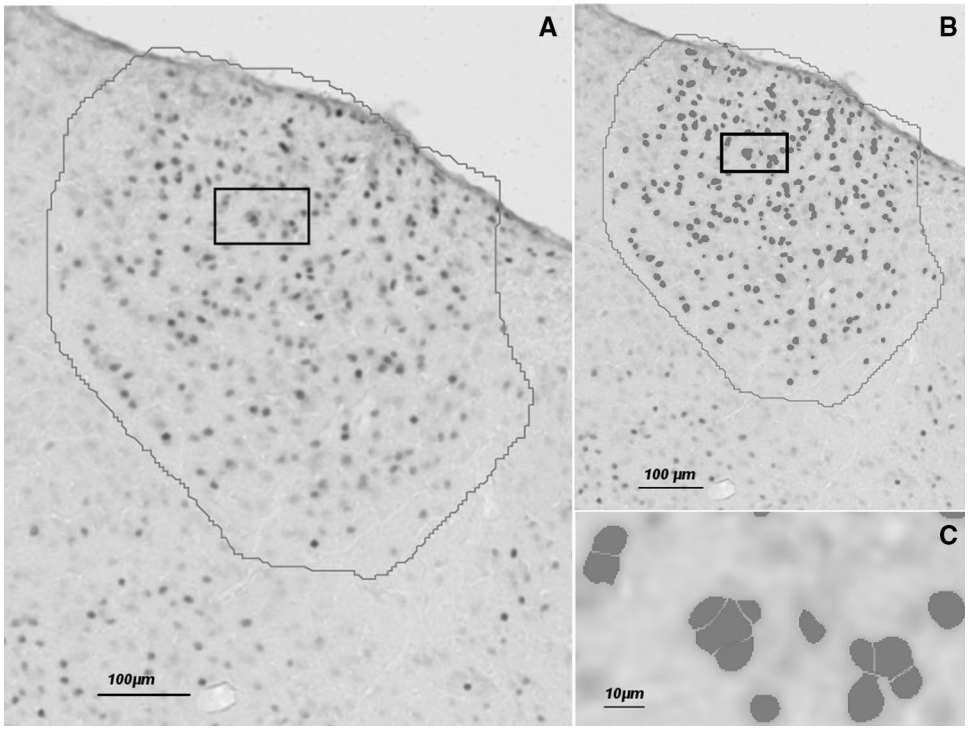

Fig. 3 Automatic counting of positive immunoreactions. The figure shows an example of the automatic counting of the left thalamic antero-dorsal nucleus, in a coronal brain section stained for c-Fos. **a** "Intensity" channel of the HSI (hue–saturation–intensity) digital system. The area of interest (grey lines) was manually drawn by the experimenter, referring directly to the rat brain atlas. **b** c-Fos-positive cell nuclei, represented by superimposed grey mark, are defined by means of a customized procedure in Image-Pro-Analyzer software (see text for details). **c** Magnification of clusters of c-Fos-positive cell nuclei of the sub-area marked by black rectangles in both **a** and **b**

(4) R5-E24 vs C5; (5) R5-E48 vs C5; (6) R5-E24 vs E24; (7) R5-E48 vs E48; (8) (R5-E24/R5-E48) vs (E24/ E48).

Significance levels were pre-set at $P < 0.05$ and determined by means of the modified t statistics (t*). The significant level was corrected, in all the non-orthogonal comparisons, according to the sequential Bonferroni's method (Holm 1979; Wallenstein et al. 1980). To compare left vs right nuclei of the thalamic structures studied bilaterally, a paired t statistic was used, taking into consideration separately each experimental condition, to avoid biases in the resulting sample variances.

Results

Wake–sleep study

A typical daily distribution of the time spent in WS states, expressed as the percentage (mean ± SEM) of the respective phase of the 12h:12-h LD cycle, was observed in the control condition (baseline): (1) light: wake, 26.3 ± 2.0; NREMS, 63.7 ± 1.8; REMS, 10.0 ± 0.7; (2) dark: wake, 75.8 ± 1.5; NREMS, 21.1 ± 1.5; REMS, 3.2 ± 0.2. Also, the levels of Delta power density of NREMS, expressed as the percentage (mean ± SEM) of the 24 h level (baseline), were larger during the L period than during the D period: (1) Light: 102.0 ± 1.0; (2) Dark: 94.0 ± 2.8.

Figure 4 shows the changes in WS states and in the Delta power density of NREMS observed in the behavioral set of the five experimental conditions of the study. Data of WS amounts are expressed in seconds as differential with respect to their distinctive baseline. It may be seen that the overall pattern of the loss of sleep time was paralleled by that of the increase in wakefulness for the entire 2 days of exposure at T_a − 10 °C. Such a tonic effect of T_a is also evidenced by either the neat opposition of the occurrence of wake and NREMS, with respect to the rest (L) and activity (D) cycle or the continuous permanence below baseline of REMS time and the Delta power density of NREMS, the two distinctive parameters of sleep homeostasis.

The recovery period following deprivation starts with the return of animals to n-lab Ta, from T_a − 10 °C. This change coincided with the onset of the L period of the LD cycle. With respect to this kind of studies, it is well known that this coincidence enhances the grooming activity that rodents display around the timing of the LD switch. This explains the excess of waking and the lack of sleep observed in the first hour of the recovery period. However, the recovery of sleep starts around the beginning of the second hour in the appropriate form of an increase in the amount of both REMS and Delta power density of NREMS.

Immunohistochemistry study

For both c-Fos and P-CREB immunoreactivity levels, no statistically significant differences were found comparing "left vs. right" parts of the bilateral (VA, AV, AD, and MD) thalamic structures (data not shown). Therefore, results are

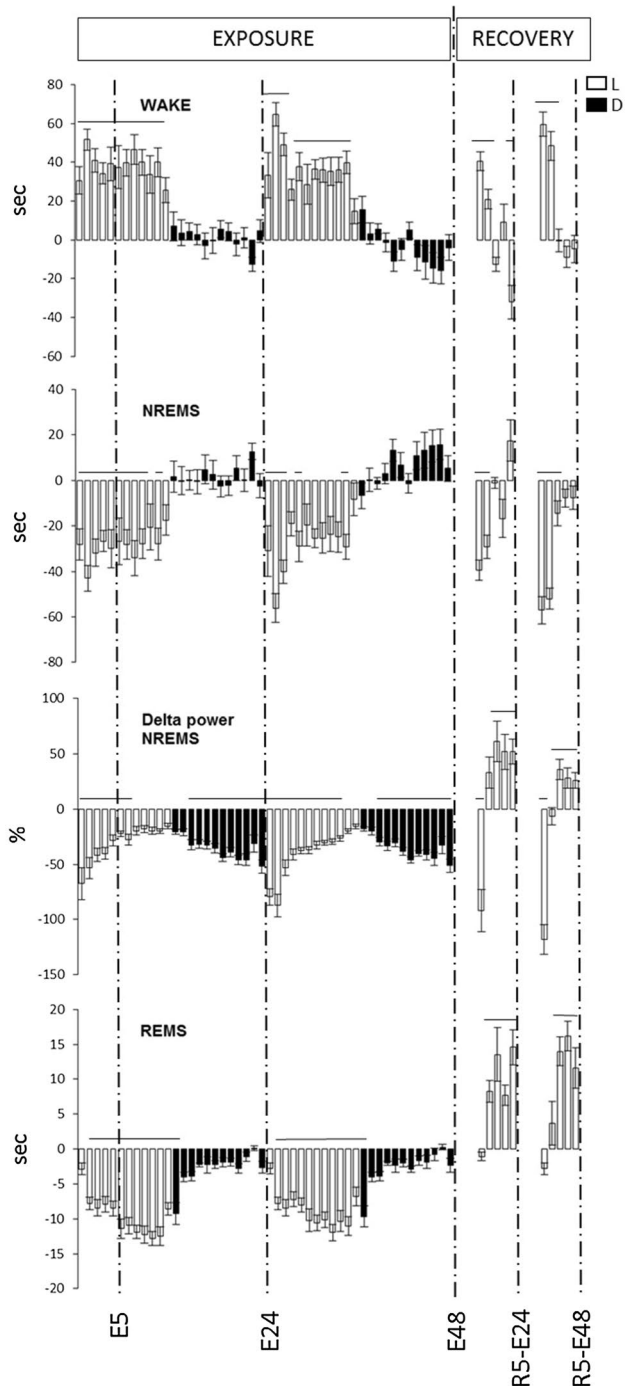

Fig. 4 Amount of wake–sleep states and the EEG Delta (0.5–4.5 Hz) power density in NREMS during a 48-h exposure to T_a − 10 °C ($n=10$) and the recovery period at n-lab T_a which followed either 24 h ($n=6$) or 48 h ($n=10$) of exposure. The histograms show the hourly difference (mean ± SEM), with respect to the appropriate baselines, of (1) the time (s) spent in wake, NREMS and REMS; (2) the percent of Delta power density in NREMS. White histograms represent light periods and black histograms represent dark periods of the day. Horizontal lines above histograms show statistically significant differences in respect to baseline ($P<0.05$). The vertical broken lines indicate the timing of the five experimental conditions selected for the immunohistochemistry study (E5, E24, E48: 5, 24 and 48 h of exposure at T_a − 10 °C, respectively; R5E24, R5-E48: 5 h of recovery at n-lab T_a following 24 h or 48 h, respectively, of exposure at T_a − 10 °C)

considered as a single mean (left/right) value for every coronal section.

c-Fos expression

As shown in Fig. 5, in the AV, AD and VA nuclei, the number of c-Fos-immunoreactive neurons (IRNs) in animals which were kept at n-lab T_a (Controls) was significantly higher when they were killed at 09:00 h, i.e., Light onset (C24 group) than at 14:00 h, i.e., 5 h after Light onset (C5 group) (C24 vs C5: $P=0.0022$ for VA; $P<0.0001$, for AV; $P<0.0001$, for AD). No statistically significant changes between the two Control groups were observed in both MD and PVN.

The largest effects of the exposure to low T_a and the following recovery at n-lab T_a were observed in the AD nucleus. In particular, the c-Fos-IRNs levels were significantly higher in animals which were exposed to low T_a for 5 h (E5) than in their time-matched Controls (E5 vs C5, $P=0.0105$). An opposite effect was observed in animals which underwent a long-term exposure since c-Fos-IRNs levels were significantly lower in both E24 and E48 experimental groups than in their time-matched Controls (E24/E48 vs C24: $P=0.0197$). Finally, although no significant changes were observed between the two groups of animals which were allowed to recover at n-lab T_a following cold exposure (R5-E24/R5-E48) and their time-matched Controls (C5), the c-Fos-IRNs levels were significantly lower in the R5-E24/R5-E48 than in the E24/E48 groups ($P=0.0025$) and in R5-E24 than in E24 ($P=0.0015$).

In the AV and VA nuclei, the pattern of changes in the number of c-Fos-IRNs induced by the exposure to low T_a was similar to that observed in AD. However, in both nuclei, no statistically significant changes were observed following the short-term exposure to low T_a (E5 vs C5, ns. for both nuclei). A large decrease in c-Fos-IRNs levels was observed in both the E24 and the E48 groups compared to their time-matched Controls (C24), when the two Exposure conditions were considered either as a whole (E24/E48 vs C24: $P<0.0001$, for VA; $P=0.0004$, for AV) or separately (E24 vs C24: $P=0.010$, for VA; $P=0.0009$, for AV; E48 vs C24: $P=0.006$, for VA; $P=0.0009$, for AV) Finally, in both nuclei, no significant differences in the number of c-Fos-IRNs were observed between the two groups of animals which were allowed to recover at n-lab T_a after the exposure to low T_a (R5E24/R5E48) and either their matched Control group (C5) or, differently from what observed in AD, the corresponding Exposure conditions (E24/E48).

In both MD and PVN nuclei, no statistically significant effects of short or long-term exposure to low T_a and of the following recovery at n-lab T_a on c-Fos-IRNs levels were observed.

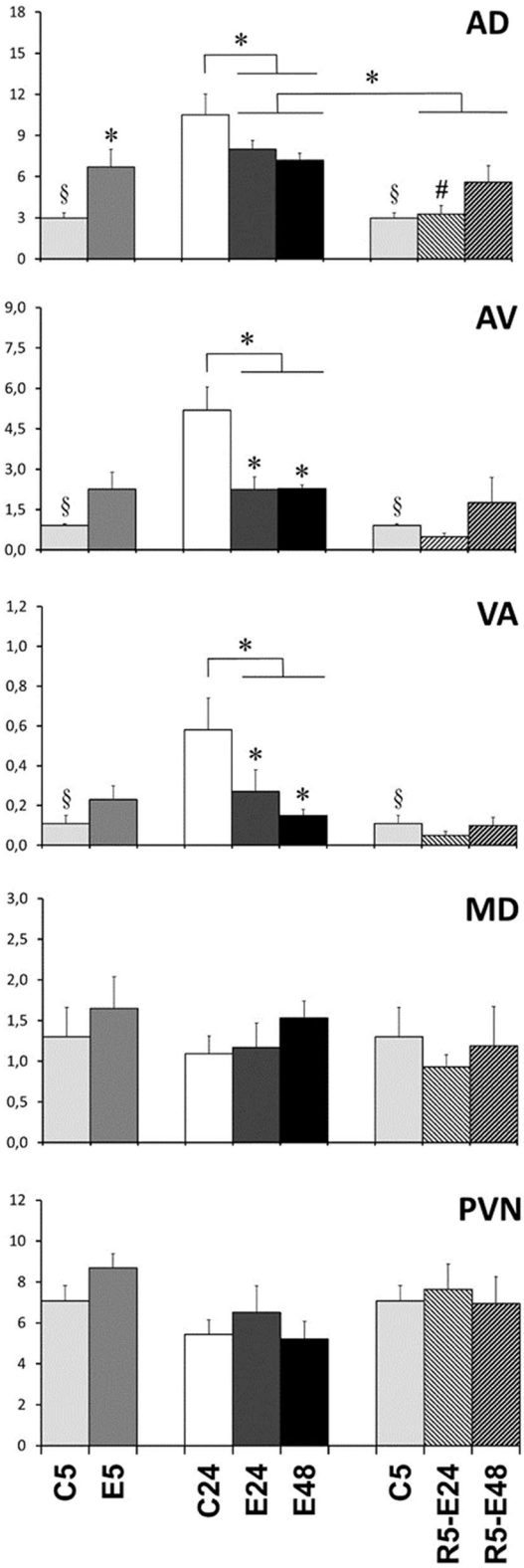

Fig. 5 Number of c-Fos-IRNs normalized per 100μm^2. Histograms and error bars represent mean ± S.E.M, respectively. Considering the timing of light-on (i.e., 9:00 AM), the following experimental conditions are shown: C24 ($n=3$) and C5 ($n=3$), 24 h and 5 h, respectively, at n-lab Ta; E5 ($n=3$), E24 ($n=3$) and E48 ($n=3$), 5 h, 24 h and 48 h, respectively, at T_a − 10 °C; R5-E24 ($n=3$) and R5-E48 ($n=3$), 5 h at n-lab Ta, following 24 h and 48 h, respectively, at T_a − 10 °C. *VA* thalamic ventral-anterior nuclei, *AV* thalamic antero-ventral nuclei, *AD* thalamic antero-dorsal nuclei, *MD* thalamic mediodorsal nuclei, *PVN* thalamic paraventricular nucleus. Statistically significant differences are also shown: $^{*}P<0.05$ vs relative control; $^{\S}P<0.05$ C5 vs C24; $^{\#}P<0.05$ recovery vs exposure

P-CREB expression

The normalized number of P-CREB-IRNs expression in the analyzed thalamic nuclei is shown in Table 1. The expression of this antigen showed no significant variations throughout the whole experimental protocol in the five thalamic nuclei.

Discussion

The results of the present study show that an intense thermoregulatory challenge caused a significant increase in c-Fos expression only in the anterior part of the thalamus, namely the AD, AV and VA nuclei, but not in MD and PVN. Also, P-CREB expression did not show any significant modification in all the nuclei examined. The pattern of sleep deprivation and recovery emerging from the results, in particular the near complete abolition of REMS at low T_a as far as autonomic activity is concerned (Parmeggiani 2003), emphasizes the suitability of the experimental model we have adopted on the ground of the functional traits of the sympathetic activation and increase in waking.

At n-lab Ta, c-Fos expression in AD, AV, and VA manifested a clear tendency to a day-night fluctuation, as shown by its large enhancement when the determination was made soon after light on (C24) rather than 5 h later (C5). This change is coherent with what observed in different brain areas of the rat in several studies in which the day-night pattern of c-Fos expression was assessed (Grassi Zucconi et al. 1993; Cirelli et al. 1993; Pompeiano et al. 1995). In accordance with the interpretation of the results by the authors of the aforementioned studies, the observed variations may be the likely result of the behavioral activation (active waking) which occurs in the late Dark period in laboratory rodents. In fact, the peak expression of c-Fos marks events occurring 1–2 h earlier (Kovács 2008). Reciprocally, c-Fos expression is apparently at its minimum during the early light period, when the EEG slow wave activity of NREMS is at its highest daily level (Tobler et al. 1992). Accordingly, opposite variations have been observed in the Cluster subdivision of the ventrolateral preoptic nucleus (Saper et al. 2005; Dentico et al. 2009), which is known to play an active and specific role in promoting sleep (Szymusiak et al. 1998, 2007).

In the first hours of cold exposure (E5), the expression of c-Fos in AD, AV and VA increased above the corresponding

Table 1 Number of P-CREB-IRNs normalized per 100μm^2

	VA	AV	AD	MD	PVN
C5	7.57 ± 0.88	14.36 ± 2.14	17.97 ± 1.29	12.15 ± 1.92	22.09 ± 1.05
E5	7.87 ± 0.58	14.02 ± 1.49	18.80 ± 1.19	12.43 ± 0.75	17.99 ± 1.61
C24	6.61 ± 1.19	10.64 ± 2.94	14.44 ± 2.69	6.69 ± 1.33	10.86 ± 1.05
E24	5.50 ± 1.52	11.65 ± 3.61	13.60 ± 3.42	6.59 ± 1.85	15.10 ± 4.26
E48	5.83 ± 0.77	10.80 ± 1.35	13.33 ± 1.91	7.09 ± 1.33	13.23 ± 5.10
R5-E24	3.66 ± 0.93	6.63 ± 2.57	11.42 ± 2.33	6.93 ± 2.18	15.64 ± 5.26
R5-E48	5.21 ± 1.69	10.05 ± 3.04	13.91 ± 3.17	8.62 ± 2.07	15.56 ± 3.52

Data are expressed as mean ± SEM. Considering the timing of light-on (i.e., 9:00 AM), the following experimental conditions are shown: C24 ($n = 3$) and C5 ($n = 3$), 24 h and 5 h, respectively, at n-lab Ta; E5 ($n = 3$), E24 ($n = 3$) and E48 ($n = 3$), 5 h, 24 h and 48 h, respectively, at low T_a (− 10.0 ± 1.0 °C); R5-E24 ($n = 3$) and R5-E48 ($n = 3$), 5 h at n-lab Ta, following 24 h and 48 h, respectively, at low Ta. No statistically significant differences among the different experimental conditions were observed

VA thalamic ventral-anterior nuclei, *AV* thalamic antero-ventral nuclei, *AD* thalamic antero-dorsal nuclei, *MD* thalamic medio-dorsal nuclei, *PVN* thalamic paraventricular nucleus

control levels (C5), although it reached the statistical significance only in AD. In addition, at the end of each of the daily periods of cold exposure (E24 and E48), the levels of c-Fos expression in AD, AV, and VA were substantially the same observed in the early hours (E5), but significantly lower than those of the corresponding control (C24). Thus, the exposure to low T_a induced a degree of activation of these nuclei that lies in between the levels of activation of C5 and C24 and is irrespective of the effects of the extent of sleep deprivation and autonomic activation. This kind of autonomy from wake–sleep and autonomic processes is also displayed by the return of c-Fos immunoreactivity to the control levels during the recovery. This suggests that the observed changes in c-Fos expression are related to the levels of behavioral activation induced by the adaptive response to changes in ambient conditions (Jankowsky et al. 2013). Thus, the hypothesis of specific involvement of these nuclei in either thermal, viz. autonomic regulations or the accrual of a sleep debt, viz. a symmetrical excess in waking (Amici et al. 1998; Cerri et al. 2005) is not supported by our data.

As clearly shown in Fig. 4, the return to n-lab T_a following either 24 or 48 h of exposure to T_a − 10 °C (R5-E24, R5-E48) is characterized by a clear sleep rebound; in this condition, cFos immunoreactivity was practically maintained at the same levels observed under control conditions (C5) in the five nuclei that were examined, suggesting the absence of any specific role in sleep promotion/regulation for these thalamic structures. It must be noted that in AD only, cellular activity during the REMS and NREMS Delta power rebounds (R5-E24, R5-E48) was significantly lower than that observed under cold exposure (E24, E48). This confirms that AD activity would be in closer relationship with the levels of behavioral activation throughout our experimental protocol compared to that of AV and VA.

Overall, the changes observed in AD, AV, and VA during the long-term exposure to cold and the following recovery period went in a different, or even opposite, direction of those previously observed in the same experimental data set at VLPO and MnPO level (Dentico et al. 2009). In fact, in both VLPO and MnPO, c-Fos expression was significantly enhanced, compared to control levels, during either the prolonged exposure to low T_a (E24, E48) or the REMS and NREMS Delta power rebounds occurring after the return to n-lab T_a (R5E24, R5-E48) (Dentico et al. 2009). In particular, a specific enhancement in c-Fos expression was found in both R5-E24 and R5-E48 at the level of the VLPO T-Cluster, an area which has been proposed to give a better demarcation of the cluster itself (Lu et al. 2000). Consistent with what observed at a hypothalamic level (Dentico et al. 2009), however, no changes in P-CREB immunoreactivity were observed at a thalamic level, suggesting that P-CREB is not a good marker of the changes in neuronal activity occurring under this experimental protocol.

Concerning the absence of variations in PVN across the whole experimental protocol, it must be noted that although spontaneous variations in the daily expression of c-Fos were found in PVN in previous experiments (Colavito et al. 2015), the results do not permit to reach a coherent interpretation of the possible functional role of this structure. In fact, under baseline conditions a similar day–night profile was observed in nocturnal (Novak et al. 1998) and diurnal (Novak et al. 2000) species, with a peak at Light onset and the nadir during the first half of the Dark period. These oscillations were therefore apparently mostly related to the activity of the suprachiasmatic nucleus, which is reciprocally connected with the PVN (Colavito et al. 2015), rather than to the absolute levels of arousal/active wakefulness of the animal. Indeed, a positive relationship between PVN activity and active waking was suggested by sleep deprivation studies in the rat (Cirelli et al. 1995; Semba et al. 2001). However, our different results may rest on methodological differences since we

were able to examine only the anterior part of the PVN and we used, with respect to others, different gene expression times and sleep deprivation techniques (Cirelli et al. 1995; Semba et al. 2001).

Finally, in the present study, no differences were found in MD, which does not appear, within the functional model of sleep deprivation and recovery we have adopted, to be directly involved in autonomic and sleep regulation. Although, to our knowledge, this is the first time that c-Fos is assessed in this nucleus under an experimental protocol that induces a clear-cut sleep deprivation followed by a rebound of both REMS and NREMS Delta power (Amici et al. 1994, 1998; Cerri et al. 2005; Dentico et al. 2009), this observation appears particularly relevant in the light of the interpretations of the main symptoms manifested by FFI patients (Lugaresi et al. 1986, 1998; Benarroch 1993; Benarroch and Stotz-Potter 1998; Montagna et al. 1998, 2003; Parchi et al. 1998).

This finding would appear actually in line with the scientific evidence since the role thalamic nuclei play in (1) sleep, as depicted by the work of Walter Hess (cf. Akert et al. 1952), still lies between an indirect intervention in the organization of different patterns of electrogenic activity (Coulon et al. 2012) and a more direct role in determining local sleep pattern and sleep recovery, through its centro-medial and antero-dorsal areas (Gent et al. 2018); (2) autonomic activity, acting as a relay station distributing visceral input to selected cortical representations (Beissner et al. 2013; Cechetto 2014) that are involved, with limbic subcortical centers, in affective responses (Lang 2014).

Although the results of our study would suggest that the autonomic dysregulation and sleep disruption observed in FFI patients are not a direct consequence of the early damage observed in AV and MD, they also emphasize that the sleep depression and the autonomic challenge brought about by a prolonged cold exposure are represented by a broad activity of the anterior thalamus. Thus, if one considers the extent of the cortical and subcortical connections of the anterior part of the structure (cf. Akert et al. 1952; Benarroch and Stotz-Potter 1998; Velajos et al. 1998; Coulon et al. 2012; Beissner et al. 2013; Cechetto 2014; Lang 2014; Gent et al. 2018) it may be reasonably concluded that our results actually support the hypothesis by Montagna et al. (2003) that the thalamic lesions occurring in FFI would act by disconnecting the limbic cortical areas and the brain region involved in sleep and autonomic regulation, rather than by shattering cells specifically involved in the control of these functions.

Acknowledgements This work has been supported by the Ministero dell'Università e della Ricerca Scientifica (MIUR), Italy and by the University of Bologna. The authors wish to thank Ms. Melissa Stott for reviewing the English.

Compliance with ethical standards

Conflict of interest The authors declare no conflict of interest.

Ethical approval All applicable international, national, and/or institutional guidelines for the care and use of animals were followed. All procedures performed were in accordance with the ethical standards of the institution or practice at which the studies were conducted.

References

Akert K, Koella WP, Hess R Jr (1952) Sleep produced by electrical stimulation of the thalamus. Am J Physiol 168:260–267

Amici R, Zamboni G, Perez E, Jones CA, Toni I, Culin F, Parmeggiani PL (1994) Pattern of desynchronized sleep during deprivation and recovery induced in the rat by changes in ambient temperature. J Sleep Res 3:250–256

Amici R, Zamboni G, Perez E, Jones CA, Parmeggiani PL (1998) The influence of a heavy thermal load on REM sleep in the rat. Brain Res 781:252–258

Amici R, Cerri M, Ocampo-Garcés A, Baracchi F, Dentico D, Jones CA, Luppi M, Perez E, Parmeggiani PL, Zamboni G (2008) Cold exposure and sleep in the rat: REM sleep homeostasis and body size. Sleep 31(5):708–715. https://doi.org/10.1093/sleep/31.5.708

Amici R et al (2014) Sleep and bodily functions: the physiological interplay between body homeostasis and sleep homeostasis. Arch Ital Biol 152:66–78

Beissner F, Meissner K, Bär KJ, Napadow V (2013) The autonomic brain: an activation likelihood estimation meta-analysis for central processing of autonomic function. J Neurosci 33:10503–10511

Benarroch EE (1993) The central autonomic network: functional organization, dysfunction, and perspective. Mayo Clin Proc 68:988–1001

Benarroch EE, Stotz-Potter EH (1998) Dysautonomia in fatal familial insomnia as an indicator of the potential role of the thalamus in autonomic control. Brain Pathol 8:527–530

Cechetto DF (2014) Cortical control of the autonomic nervous system. Exp Physiol 99:326–331

Cerri M et al (2005) Cold exposure and sleep in the rat: effects on sleep architecture and the electroencephalogram. Sleep 28:694–705

Cirelli C, Pompeiano M, Tononi G (1993) Fos-like immunoreactivity in the rat brain in spontaneous wakefulness and sleep. Arch Ital Biol 131:327–330

Cirelli C, Pompeiano M, Tononi G (1995) Sleep deprivation and c-fos expression in the rat brain. J Sleep Res 4:92–106

Colavito V, Tesoriero C, Wirtu AT, Grassi-Zucconi G, Bentivoglio M (2015) Limbic thalamus and statedependent behavior: The paraventricular nucleus of the thalamic midline as a node in circadian timing and sleep/wake-regulatory networks. Neurosci Biobehav Rev 54:3–17

Coulon P, Budde T, Pape HC (2012) The sleep relay-the role of the thalamus in central and decentral sleep regulation. Pflugers Arch 463:53–71

Dentico D et al (2009) c-Fos expression in preoptic nuclei as a marker of sleep rebound in the rat. Eur J Neurosci 30:651–661

Garcia-Munoz M, Arbuthnott GW (2015) Basal ganglia-thalamus and the "crowning enigma". Front Neural Circuits 9:71

Gent TC, Bandarabadi M, Gutierrez Herrera C, Adamantidis AR (2018) Thalamic dual control of sleep and wakefulness. Nat Neurosci 21:974–984

Grassi-Zucconi G et al (1993) c-fos mRNA is spontaneously induced in the rat brain during the activity period of circadian cycle. Eur J Neurosci 5:1071–1078

Holm S (1979) A simple sequentially rejective multiple test procedure. Scand J Stat 6:65–70
Imeri L, Moneta ME, Mancia M (1988) Changes in spontaneous activity of medialis dorsalis thalamic neurones during sleep and wakefulness. Electroencephalogr Clin Neurophysiol 69:82–84
Jankowski MM et al (2013) The anterior thalamus provides a subcortical circuit supporting memory and spatial navigation. Front Syst Neurosci 30:7–45
Kovács KJ (2008) Measurement of immediate-early gene activation-c-fos and beyond. J Neuroendocrinol 20:665–672
Lang PJ (2014) Emotion's response patterns: the brain and the autonomic nervous system. Emot Rev 6:93–99
Lu J, Greco MA, Shiromani P, Saper CB (2000) Effect of lesions of the ventrolateral preoptic nucleus on NREM and REM sleep. J Neurosci 20:3830–3842
Lugaresi E et al (1986) Fatal familial insomnia and dysautonomia with selective degeneration of thalamic nuclei. N Engl J Med 315:997–1003
Lugaresi E, Tobler I, Gambetti P, Montagna P (1998) The pathophysiology of fatal familial insomnia. Brain Pathol 8:521–526
Luppi M et al (2010) Hypothalamic osmoregulation is maintained across the wake–sleep cycle in the rat. J Sleep Res 19:394–399
Marini G, Gritti I, Mancia M (1988a) Ibotenic acid lesions of the thalamic medialis dorsalis nucleus in the cat: effects on the sleep-waking cycle. Neurosci Lett 89:259–264
Marini G, Gritti I, Mancia M (1988b) Changes in sleep–waking cycle induced by lesions of medialis dorsalis thalamic nuclei in the cat. Neurosci Lett 85:223–227
Martelli D et al (2014) The direct cooling of the preoptic-hypothalamic area elicits the release of thyroid stimulating hormone during wakefulness but not during REM sleep. PLoS One 9:e87793
McKinley MJ, Yao ST, Uschakov A, McAllen RM, Rundgren M, Martelli D (2015) The median preoptic nucleus: front and centre for the regulation of body fluid, sodium, temperature, sleep and cardiovascular homeostasis. Acta Physiol (Oxf) 214:8–32
Montagna P et al (1998) Clinical features of fatal familial insomnia: phenotypic variability in relation to a polymorphism at codon 129 of the prion protein gene. Brain Pathol 8:515–520
Montagna P, Gambetti P, Cortelli P, Lugaresi E (2003) Familial and sporadic fatal insomnia. Lancet Neurol 2:167–176
Morrrison SF (2016) Central neural control of thermoregulation and brown adipose tissue. Auton Neurosci 196:14–24
Novak CM, Nunez AA (1998) Daily rhythms in Fos activity in the rat ventrolateral preoptic area and midline thalamic nuclei. Am J Physiol Regul Integr Comp Physiol 275:R1620–R1626
Novak CM, Smale L, Nunez AA (2000) Rhythms in Fos expression in brain areas related to the sleep-wake cycle in the diurnal Arvicanthis niloticus. Am J Physiol Regul Integr Comp Physiol 278:R1267–R1274
Parchi P et al (1998) Molecular pathology of fatal familial insomnia. Brain Pathol 8:539–548
Parmeggiani PL (2003) Thermoregulation and sleep. Front Biosci 8:s557–s567
Paxinos G, Watson C (2007) The rat brain in stereotaxic coordinates. VI edn. Academic Press, Sydney
Pompeiano M, Cirelli C, Arrighi P, Tononi G (1995) c-Fos expression during wakefulness and sleep. Neurophysiol Clin 25:329–341
Saper CB, Scammell TE, Lu J (2005) Hypothalamic regulation of sleep and circadian rhythms. Nature 437:1257–1263
Semba K, Pastorius J, Wilkinson M, Rusak B (2001) Sleep deprivation-induced c-fos and junB expression in the rat brain: effects of duration and timing. Behav Brain Res 120:75–86
Sheroziya M, Timofeev I (2014) Global intracellular slow-wave dynamics of the thalamocortical system. J Neurosci 34:8875–8893
Steriade M, Jones EG, McCormick DA (1997) Thalamus, vol 1. Elsevier, Oxford
Stotz-Potter E, Benarroch EE (1998) Removal of GABAergic inhibition in the mediodorsal nucleus of the rat thalamus leads to increases in heart rate and blood pressure. Neurosci Lett 247:127–130
Szymusiak R, Alam N, Steininger TL, McGinty D (1998) Sleep–waking discharge patterns of ventrolateral preoptic/anterior hypothalamic neurons in rats. Brain Res 803:178–188
Szymusiak R, Gvilia I, McGinty D (2007) Hypothalamic control of sleep. Sleep Med 8:291–301
Tobler I, Franken P, Trachsel L, Borbély AA (1992) Models of sleep regulation in mammals. J Sleep Res 1:125–127
Tsanov M et al (2011) Oscillatory entrainment of thalamic neurons by theta rhythm in freely moving rats. J Neurophysiol 105:4–17
van Groen T, Kadish I, Michael Wyss J (2002) Role of the anterodorsal and anteroventral nuclei of the thalamus in spatial memory in the rat. Behav Brain Res 132:19–28
Van der Werf YD, Witter MP, Groenewegen HJ (2002) The intralaminar and midline nuclei of the thalamus. Anatomical and functional evidence for participation in processes of arousal and awareness. Brain Res Rev 39:107–140
Velajos JL, Oliva M, Alfageme F (1998) Afferent projections to the mediodorsal and anterior Thalamic nuclei in the cat. Anatomical-clinical correlations. Brain Pathol 8:549–552
Vertes RP, Linley SB, Hoover WB (2015) Limbic circuitry of the midline thalamus. Neurosci Biobehav Rev 54:89–107
Wallenstein S, Zucker CL, Fleiss JL (1980) Some statistical method useful in circulation research. Circ Res 47:1–9
Wolff M, Alcaraz F, Marchand AR, Coutureau E (2015) Functional heterogeneity of the limbic thalamus: From hippocampal to cortical functions. Neurosci Biobehav Rev 54:120–130
Zamboni G et al (2004) Specific changes in cerebral second messenger accumulation underline REM sleep inhibition induced by the exposure to low ambient temperature. Brain Res 1022:62–70